Global Journal of Researches in Engineering
Mechanical andMechanicsEngineering
Volume 13 Issue 11 Version 1.0 Year 2013
Type: Double Blind Peer Reviewed International Research Journal
Publisher: Global Journals Inc. (USA)
Online ISSN:2249-4596Print ISSN:0975-5861

Conjugate Cooling of a Protruding Heater in a Channel with Distinct Flow Constraints

By Thiago Antonini Alves & Carlos A.C. Altemani
Universidade Tecnológica Federal do Paraná - UTFPR/Ponta Grossa, Brazil

Abstract- The conjugate cooling of a single block heater mounted on a conductive wall of a parallel plates channel was investigated under distinct laminar airflow constraints: fixed flow rate, fixed channel flow pressure drop and fixed pumping power. The heater was cooled by direct forced convection to the airflow and by conduction through its contact with the channel wall. The investigation was performed for a twodimensional configuration with fixed channel geometry and variable heater height. At the channel entrance the flow velocity and temperature were uniform. The channel wall thickness was constant and its thermal conductivity ranged from 0 to 80 that of the air, while the heater thermal conductivity was equal to 500 that of the air. The conservation equations were solved numerically by the control volumes method with the SIMPLE algorithm. The results were expressed in dimensionless form, considering the three distinct flow constraints. For a fixed flow rate, the heater temperature always decreased as the heater height increased. For the other two flow constraints, there is a critical relative heater height which minimizes its thermal resistance to the airflow. The results also indicated that for a conductive substrate, the conduction from the heater to the substrate plate cannot be neglected in comparison to the direct convective cooling to the airflow.

GJRE-A Classification : *FOR Code: 290501*

Conjugate Cooling of a Protruding Heater in a Channel with Distinct Flow Constraints

Thiago Antonini Alves [α] & Carlos A.C. Altemani [σ]

Abstract- The conjugate cooling of a single block heater mounted on a conductive wall of a parallel plates channel was investigated under distinct laminar airflow constraints: fixed flow rate, fixed channel flow pressure drop and fixed pumping power. The heater was cooled by direct forced convection to the airflow and by conduction through its contact with the channel wall. The investigation was performed for a two-dimensional configuration with fixed channel geometry and variable heater height. At the channel entrance the flow velocity and temperature were uniform. The channel wall thickness was constant and its thermal conductivity ranged from 0 to 80 that of the air, while the heater thermal conductivity was equal to 500 that of the air. The conservation equations were solved numerically by the control volumes method with the SIMPLE algorithm. The results were expressed in dimensionless form, considering the three distinct flow constraints. For a fixed flow rate, the heater temperature always decreased as the heater height increased. For the other two flow constraints, there is a critical relative heater height which minimizes its thermal resistance to the airflow. The results also indicated that for a conductive substrate, the conduction from the heater to the substrate plate cannot be neglected in comparison to the direct convective cooling to the airflow.

I. Introduction

The space available for electronic components mounted on circuit boards may sometimes be restricted and their cooling must be obtained by airflow with moderate velocities. Under these conditions, there may not be enough room to install a finned heat sink on the components with high heat dissipation rates. In this case, the thermal design may benefit from the conjugate forced convection-conduction cooling of a heated component.

Two extensive reviews of the literature on the conjugate forced convection-conduction heat transfer in electronic equipment were presented by Ortega [1] and Nakayama [2]. A modeling hierarchy for heat transfer study was adopted, involving both flush mounted heat sources (e.g., Ramadhyani et al. [3]) and protruding two-dimensional heat sources (e.g., Davalath and Bayazitoglu [4]). In this case, distinct investigations considered either periodically fully developed flow and heat transfer (e.g., Kim and Anand [5]) or a developing flow and heat transfer (e.g., Kim and Anand [6]). Nakayama and Park [7] presented an investigation of the conjugate heat transfer from a single three-dimensional heater mounted on the wall of a rectangular channel with a 16:1 aspect ratio. Their experimental measurements, considering air velocities in the range from 1 to 7 m/s, were employed to set the boundary conditions for a numerical analysis of the conduction in the duct wall. From their data they derived a correlation for the direct convective heat transfer from the heated block to the airflow, but they pointed out that it did not agree with the predictions of previous correlations from the literature. As a consequence, they indicated the need for more work to obtain a correlation of wider applicability, even for the direct heat transfer from the block. Nakamura and Igarashi [8] performed an experimental investigation to obtain a general correlation of the Nusselt number for a heated low-profile block placed in a rectangular duct. The correlation was shown to be applicable regardless of the configuration of the block and duct, expressed in terms of a modified Reynolds number, under conditions of laminar flow, a low profile block and a low blockage effect. Due to these restrictions, it seems that even the direct convective heat transfer from a single heated block may still be considered an open problem to further research. When it comes to more than one heater mounted on a wall, several investigations presented in the recent literature were related to the thermal optimization, in which the heaters distribution usually is an important parameter. Silva et al. [9] considered two analytical approaches to optimize the distribution of heat sources flush mounted on a wall cooled by forced convection. The results were validated by a numerical investigation to distribute heat sources inside a channel formed by parallel plates. It was concluded that the heat sources should be placed nonunifomly on the wall, with the smallest distance between them near the tip of the boundary layer. This migration of the heat sources towards the tip was dependent on the Reynolds number and the heat sources length. Icoz et al. [10] presented a design methodology for air and liquid cooling systems applied to a parallel plates channel with two identical heating elements. The effects of the Reynolds number, the separation distance and the protrusion heights on the heat transfer rates from the heat sources and the channel flow pressure drop were investigated. The concurrent use of simulation and experiment was adopted in order to improve the efficiency of design optimization. The results indicated that the optimal

Author α: Av. Monteiro Lobato, km 4, CEP 85.016-204 Ponta Grossa, Paraná, Brasil,UTFPR/Ponta Grossa. e-mail: thiagoaalves@utfpr.edu.br
Author σ: Unicamp/FEM/DE. e-mail: altemani@fem.unicamp.br

values of Reynolds number, heat source height and separation distance between the heaters depend on an objective function. For air cooling, it was shown that the spacing needed to optimize the heat transfer from the downstream heater is greater than that for the upstream heater. In addition, the optimal Reynolds values for a given protrusion height were observed to be greater for the upstream heat source than the downstream source. The thermal optimization may be subjected to constraints such as the maximum component temperature, flow pressure drop or pumping power. These constraints may however also be considered even for the thermal design of a single heated component on a parallel plates channel.

The present work is concerned with the conjugate cooling of a single heater mounted on the lower wall of a two-dimensional parallel plates channel, as indicated in Fig. 1, under laminar airflow conditions. The thermal contact with the lower wall (substrate plate) was considered perfect and the energy dissipation rate per unit depth of the heater was constant. The conjugate cooling was by direct forced convection from the heater surfaces in contact with the airflow and by conduction through its contact with the substrate plate. The effects of the relative heater height in the channel, of the airflow rate and of the substrate plate thermal conductivity were considered in the analysis performed. The results will be presented considering three distinct constraints for the airflow in the channel: a specified flow rate, a fixed pressure drop and a constant pumping power. Due to the conjugate nature of the heater cooling, a dimensionless global thermal resistance was defined and presented in the results. In spite of the two-dimensional restriction of the present analysis, the heat transfer enhancement promoted by the substrate conduction was clearly identified.

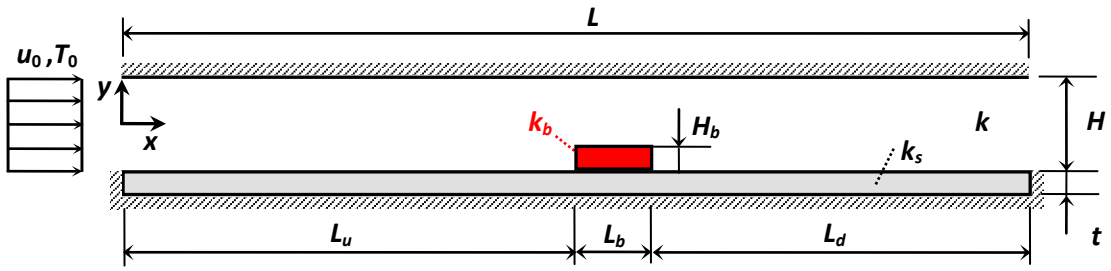

Figure 1 : Domain of the conjugate heat transfer problem

II. Analysis

a) Problem Formulation and Dimensionless Parameters

The present investigation was performed within the two-dimensional domain indicated in Fig. 1, comprising a parallel plates channel with a heater mounted on the lower wall. The channel had a fixed geometry, with height H and a total length $L = 20H$. The channel upstream length was $L_u = 10H$, the heater length $L_b = H$ and the downstream length $L_d = 9H$, as indicated in Fig. 1. The heater height H_b was a parameter of investigation, varying from zero (flush mounted heater) to a fraction ($H_b/H < 1$) of the channel height. This geometry was suggested by related works applied to the cooling of electronic components assembled on stacks of circuit boards, e.g., Davalath and Bayazitoglu [4], Nakayama [2], Zeng and Vafai [11] and Alves [12].

The heater cooling was provided by a laminar airflow with constant properties, under steady state conditions, with uniform velocity (u_0) and temperature (T_0) at the channel entrance. The corresponding Reynolds number was based on the channel hydraulic diameter,

$$Re = \frac{u_0 2H}{\upsilon} \qquad (1)$$

The channel lower wall had a thickness $t = (0.10\ H)$ and its thermal conductivity relative to the air, (k_s/k), was varied in the range from 0 to 80. Its upper surface was in contact with the channel flow and also supported the heater with perfect thermal contact. Its lower and lateral surfaces, as well as the channel upper surface, were adiabatic, as indicated in Fig. 1. The heater thermal conductivity relative to the air was (k_b/k) = 500. The heating was provided by a uniform volumetric heat generation rate within the heater, in such a way to always provide a heat generation rate equal to q'_b per unit depth normal to Fig. 1. When the heater was flush mounted, it generated a uniform heat flux along its length (L_b), such that the same heat transfer rate $q'_b = \left(q''_b L_b \right)$ was imposed.

The conservation equations of mass, momentum and energy for this combined entry length and conjugate heat transfer problem were expressed in dimensionless form. The dimensionless variables were, referred to Fig. 1, $X = x/(2H)$, $Y = y/(2H)$, $U = u/u_0$, $V = v/u_0$, $p^* = p/(\rho\ u_0^2)$, and $\theta = \left(T - T_0\right)k/q'_b$. A numerical solution procedure, to be described in the next section, employed the same form of the conservation equations in the solid and fluid regions of the domain presented in Fig. 1. In the solid regions, the artifice of very large local viscosity was used (i.e., a very small local Re), so that

the resulting local velocities were negligible. The conservation equations in dimensionless form were

$$\frac{\partial U}{\partial X}+\frac{\partial V}{\partial Y}=0 \quad (2)$$

$$U\frac{\partial U}{\partial X}+V\frac{\partial U}{\partial Y}=-\frac{\partial p*}{\partial X}+\frac{1}{Re}\left(\frac{\partial^2 U}{\partial X^2}+\frac{\partial^2 U}{\partial Y^2}\right) \quad (3)$$

$$U\frac{\partial V}{\partial X}+V\frac{\partial V}{\partial Y}=-\frac{\partial p*}{\partial Y}+\frac{1}{Re}\left(\frac{\partial^2 V}{\partial X^2}+\frac{\partial^2 V}{\partial Y^2}\right) \quad (4)$$

$$U\frac{\partial \theta}{\partial X}+V\frac{\partial \theta}{\partial Y}=\frac{1}{Re\,Pr}\frac{k^+}{C^+}\left(\frac{\partial^2 \theta}{\partial X^2}+\frac{\partial^2 \theta}{\partial Y^2}\right)+S* \quad (5)$$

Besides the uniform velocity u_0 at the flow inlet, the outflow boundary was treated with negligible diffusion for both velocity components. Along the upper and lower surfaces of the domain, both velocity components were equal to zero. The flow temperature was uniform (T_0) at the channel inlet, while the upper and lower surfaces of the domain and both ends of the substrate plate were adiabatic. At the outflow boundary, the temperature profile was obtained considering negligible diffusion. The dimensionless volumetric source term S^* indicated in Eq. (5) was not negligible only in the solid region comprised by the heater, where it was uniform, expressed by

$$S* = \left(Re\,Pr\,H_b^* L_b^* C^+ \right)^{-1} \quad (6)$$

In Eq. (5) k^+ and C^+ (6), k+ and C+ represent respectively the thermal conductivity and the unit thermal capacity (ρc) of each region relative to those of the air. The fluid Prandtl number is represented by *Pr* and the dimensionless heater height and length are respectively $H_b^* = (H_b/2H)$ and $L_b^* = (L_b/2H)$. The dimensionless volumetric source term $S*$ was always uniform in each investigated case, but it changed with the heater height and the fluid flow rate, as indicated in Eq. (6). The properties of the cooling fluid (air) were constant, taken from a table at 300 K (Kays and Crawford [13]) for the simulations performed.

The flow pressure drop $\left(\Delta p = \rho u_0^2 \Delta p*\right)$ across the channel was obtained from the average pressure distributions evaluated at the inlet and outlet channel boundaries. The flow pumping power (P'_W) was obtained by the product of the referred pressure drop and the corresponding channel volumetric flow rate. It was expressed in dimensionless form considering its ratio with the heat generation per unit heater length:

$$\frac{P'_W}{q'_b}=\left(\frac{\upsilon \Delta p}{q'_b}\right)\frac{Re}{2} \quad (7)$$

The term in parenthesis on the right side of Eq. (7) represents a dimensionless pressure drop, which will be denoted by $\Delta p^+ = \left(\upsilon \Delta p / q'_b\right)$. It is proportional to the pressure drop, since the fluid properties and the heat generation within the heater were constant. The left side of this equation represents a dimensionless pumping power, which will be denoted by $W_p^+ = \left(P'_W / q'_b\right)$.

Since all the heat generation rate will ultimately be transferred to the airflow, the heater average surface temperature along its four edges, $\overline{T}_h$, was evaluated from the local distribution in order to define a dimensionless global thermal resistance per unit depth, as follows:

$$R'_t = \frac{k\left(\overline{T}_h - T_0\right)}{q'_b} \quad (8)$$

This thermal resistance corresponds to the heater dimensionless average surface temperature, i.e., $R'_t = \overline{\theta}_h$.

b) Numerical Solution Procedure

The stated conservation equations were solved considering the conjugate domain indicated in Fig. 1, comprising the substrate plate, the heater and the flow regions. The control volumes method (Patankar [14]) was employed with the *SIMPLE* algorithm in order to obtain the flow field. A very small *Re* was imposed in all the control volumes in the solid regions, so that the resulting velocities were negligible in the substrate plate and heater. At the solid-fluid interfaces, the diffusion coefficients were evaluated by the harmonic mean in order to handle the abrupt changes of the solid to fluid properties. The mentioned boundary conditions for the flow and for the temperature distributions were imposed at the four boundaries of the domain presented in Fig. 1.

The results were obtained with a non-uniform grid deployed on the solution domain, comprising 348 control volumes in *x* -direction and 34 control volumes in the y-direction. It should be kept in mind that the channel aspect ratio was fixed, with $(L/H) = 20$, and that the lower wall thickness was related to the channel height as $(t/H) = 0.10$. In the x-direction, the grid was most refined over the heater length L_b, which contained 80 uniformly distributed control volumes. Along the upstream length L_u, 194 control volumes were uniformly deployed, and 74 others were distributed along the downstream length L_d. Along the *y* -direction, the grid was finer near the solid-fluid interfaces due to larger gradients of the dependent variables in these regions.

Several grids were tested before the final selection to obtain the numerical results. Most of the tests involving grid refinement were performed with *Re* = 1260. The number of grid points was increased until further grid refinement practically did not change the obtained results. The Richardson extrapolation technique (De Vahl Davis [15]) was employed for a particular case, indicating that the numerical error associated with the grid spacing was of second order. It was also verified that in the conductive substrate plate a uniform grid with 4 control volumes along its thickness was enough to obtain results independent of further grid refinement.

The discretization equations and their boundary conditions were solved by an iterative process based on the line-by-line method described by Patankar [14]. The solution was achieved when the absolute changes of the primitive variables in several locations were smaller than 10^{-5} between two consecutive iterations, while the global mass conservation in the domain was satisfied in all iterations. The numerical results were obtained in a microcomputer (Intel® Core™ 2 Quad Q6600 processor 2.4GHz and 4GB RAM), in about 15 minutes for a typical solution considering a conductive substrate.

III. Results and Discussion

a) Fixed Mass Flow Rate

The condition of fixed mass flow rate through the channel was specified in dimensionless form by a constant Reynolds number (*Re*). Five values of *Re* in the range from 630 to 1890 were selected in the laminar regime to present the results. They correspond, for a channel height H = 0.01 m, to u_0 in the range from 0.5 m/s to 1.5 m/s. The results will be presented in terms of a dimensionless heater height defined by $H_b^+ = (H_b/H)$, because it was felt more intuitive than $(H_b/2H)$. The dimensionless pressure drop $\Delta p^+ = \upsilon \Delta p / q'_b$ in the channel is presented in Fig. 2 as a function of the dimensionless heater height H_b^+, for the distinct values of *Re*. It shows that Δp^+ increases with both *Re* and H_b^+, due respectively to larger shear stress and an increased obstruction of the channel cross section. The heater height H_b^+ in this figure is limited to 0.40 in order to keep the flow recirculation downstream of the heater within the channel.

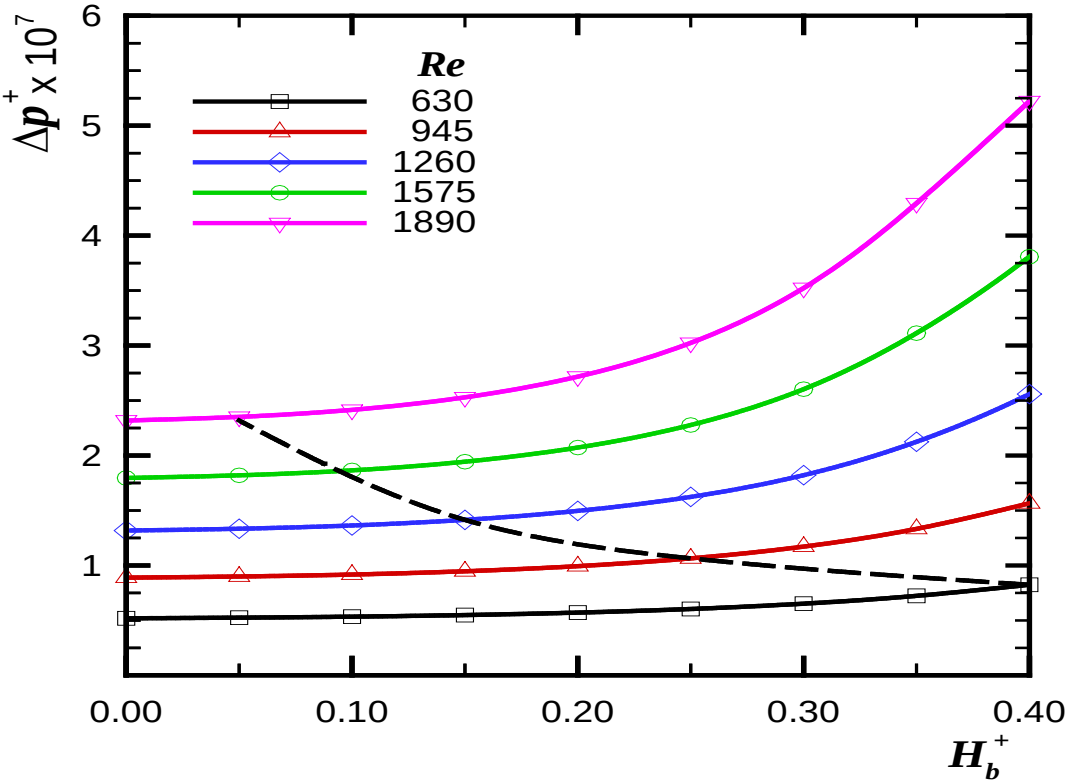

Figure 2 : Flow pressure drop for fixed flow rate

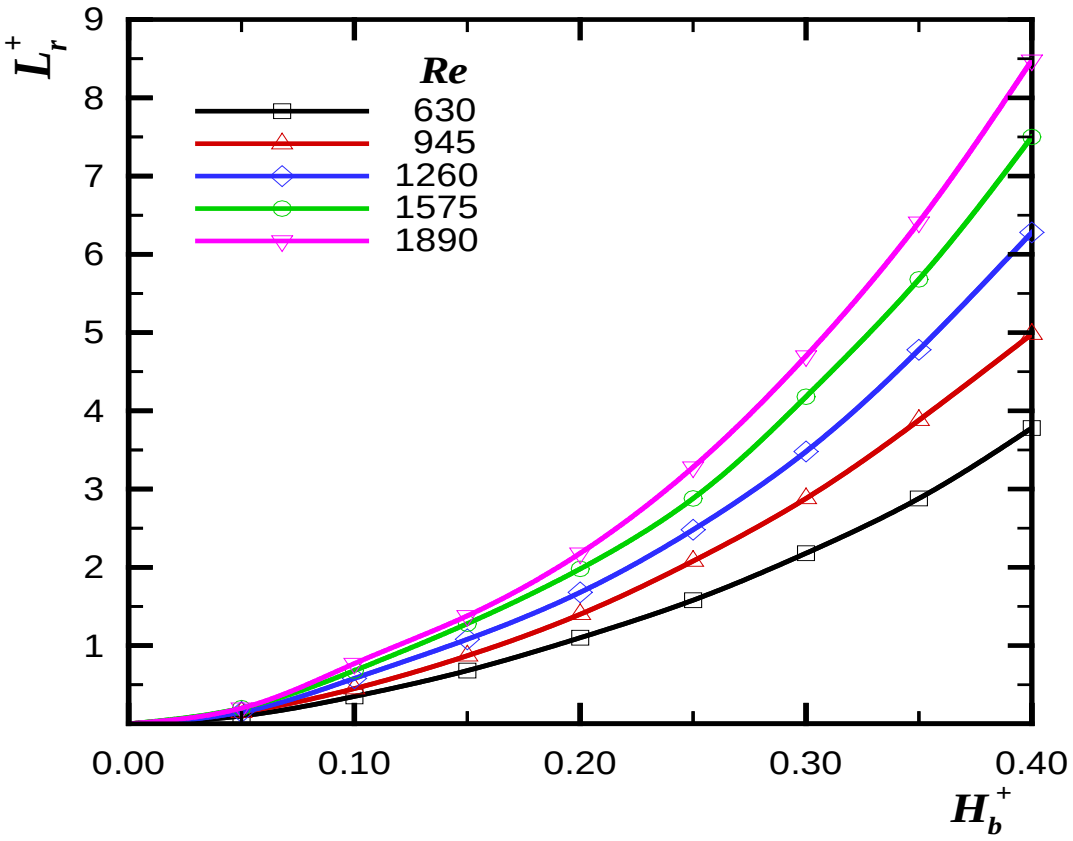

Figure 3 : Flow recirculation length downstream of the heater

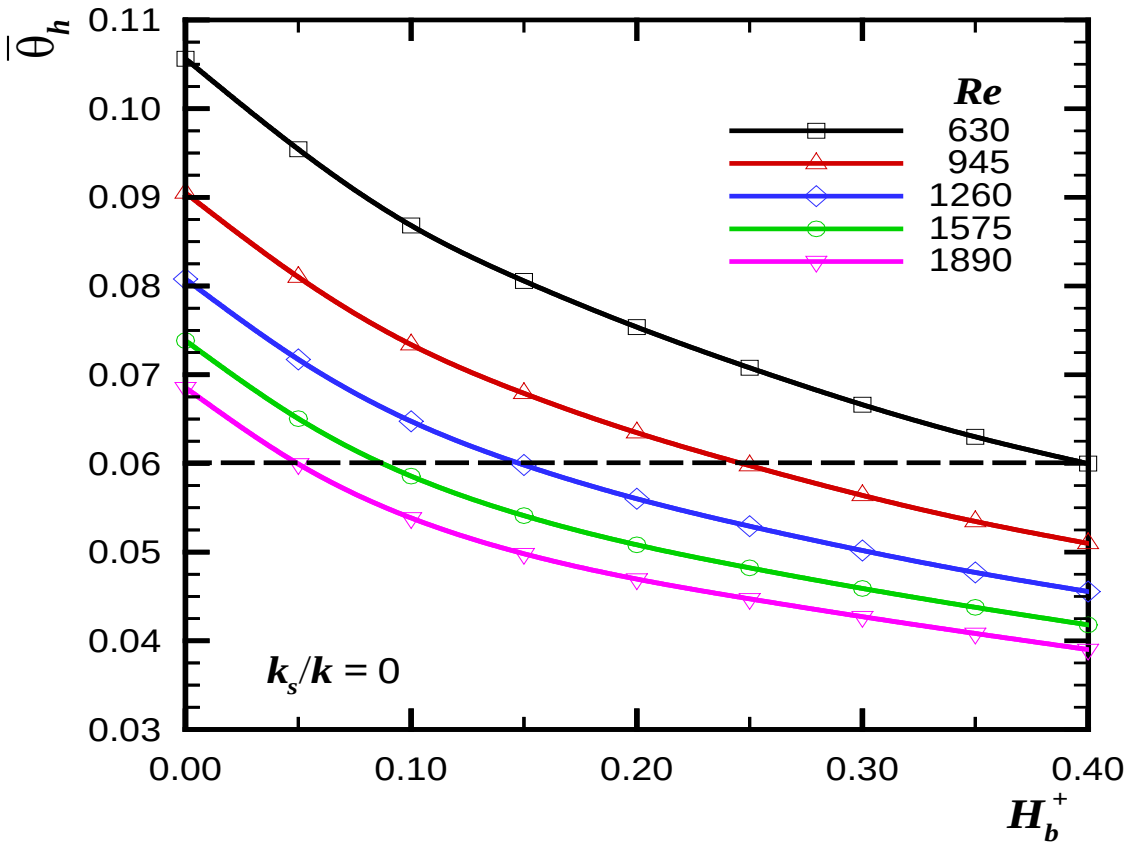

Figure 4 : Heater average temperature – fixed flow rate and $(k_s/k) = 0$

A conductive substrate wall provides a conduction heat spreader for the heater at their common interface. Thus, the heater cooling is provided by a conjugate forced convection-conduction heat transfer. The results for the heater average temperature $\overline{\theta}_h$, considering a substrate to air thermal conductivity ratio (k_s/k) = 80, are presented in Fig. 6. The effects of *Re* and the relative height H_b^+ are similar to those for the adiabatic substrate, i.e., the temperature $\overline{\theta}_h$ decreases when these parameters increase. Due however to the conjugate heat transfer, the temperature profiles in Fig. 6 are lower than those for the adiabatic substrate, as shown in Fig. 5. Considering the same heater temperature limit $\overline{\theta}_{h,max} = 0.06$ adopted for the adiabatic substrate, Fig. 6 shows that this thermal requirement would be satisfied now under any of the investigated conditions. This result indicates the remarkable contribution to thermal control due to conduction in the substrate. In this case, the flush mounted heater with the smallest airflow rate would require the minimum pumping power and pressure drop.

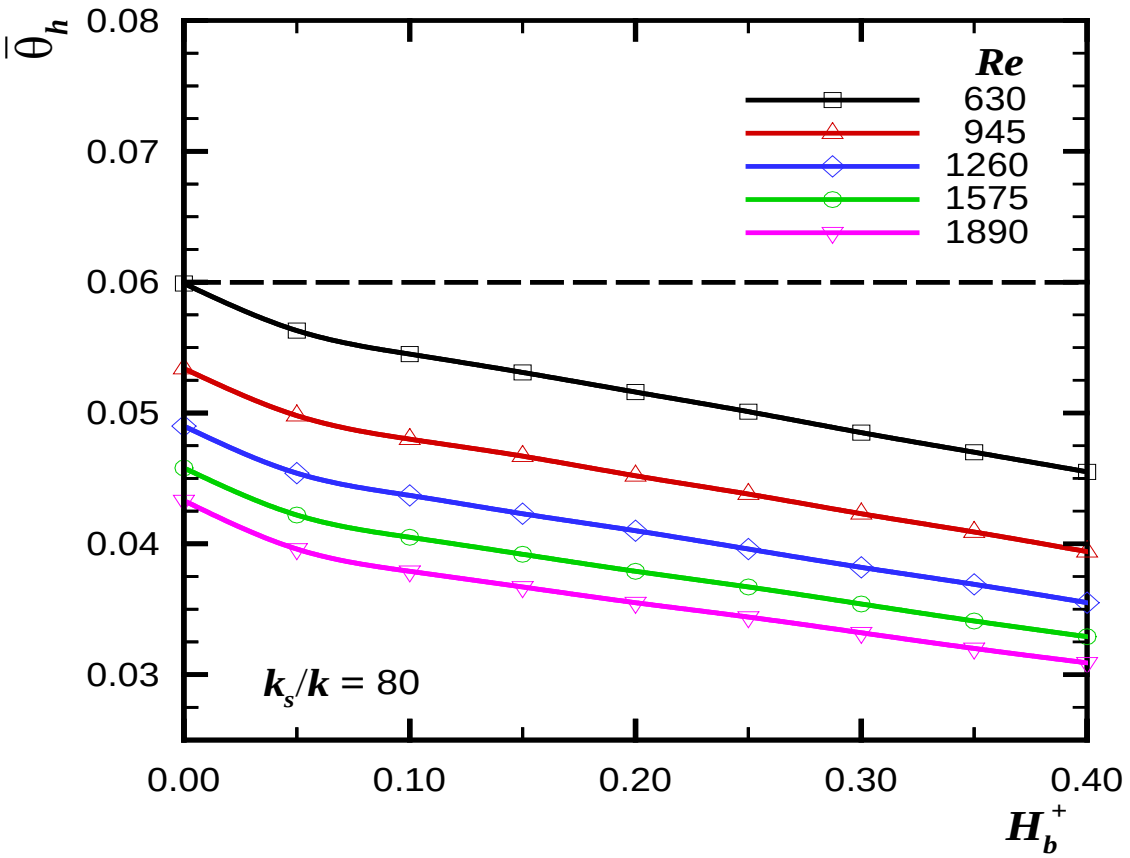

Figure 5 : Heater average temperature – fixed flow rate and (k_s/k) = 80

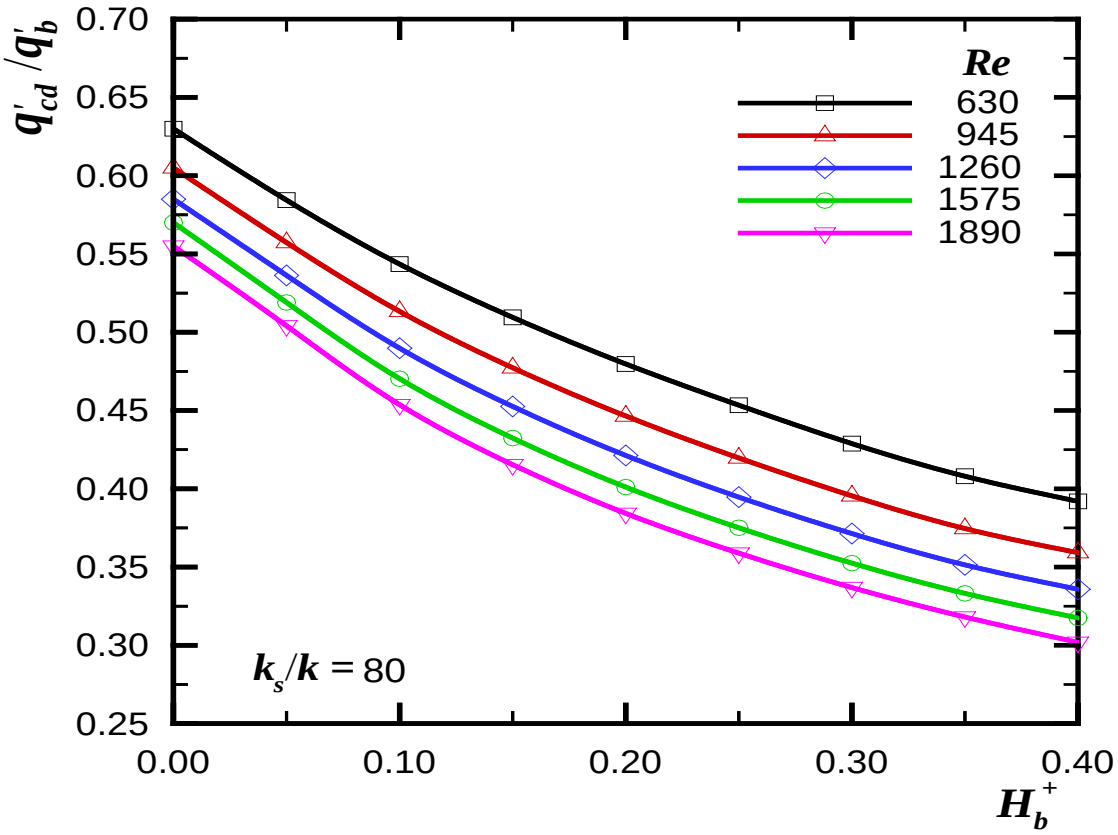

Figure 6 : Fraction of heat conduction through the substrate plate – (k_s/k) = 80

The heater conduction loss through the substrate relative to the total heat generation (q'_{cd} / q'_b) presents a trend similar to that of $\overline{\theta}_h$ with respect to *Re* and H_b^+, as shown in Fig. 6 for (k_s/k) = 80. These results also indicate that the conductive and the convective losses are of the same order and neither can be neglected. The channel flow pressure drop and the required pumping power for the conductive substrate are the same as those for the adiabatic substrate, since the flow properties are constant. An increase of the substrate thermal conductivity (k_s/k)

decreases the heater average temperature $\overline{\theta}_h$, as presented in Fig. 7 for the smallest *Re* (the largest conduction contribution). This figure also shows that the minimum heater height H_b^+ needed to keep it below the temperature limit ($\overline{\theta}_{h,max} = 0.06$) decreases as (k_s/k) increases. Thus, for (k_s/k) = 0, a height H_b^+ = 0.40 is necessary, but for (k_s/k) = 80, the heater may be flush mounted on the substrate plate.

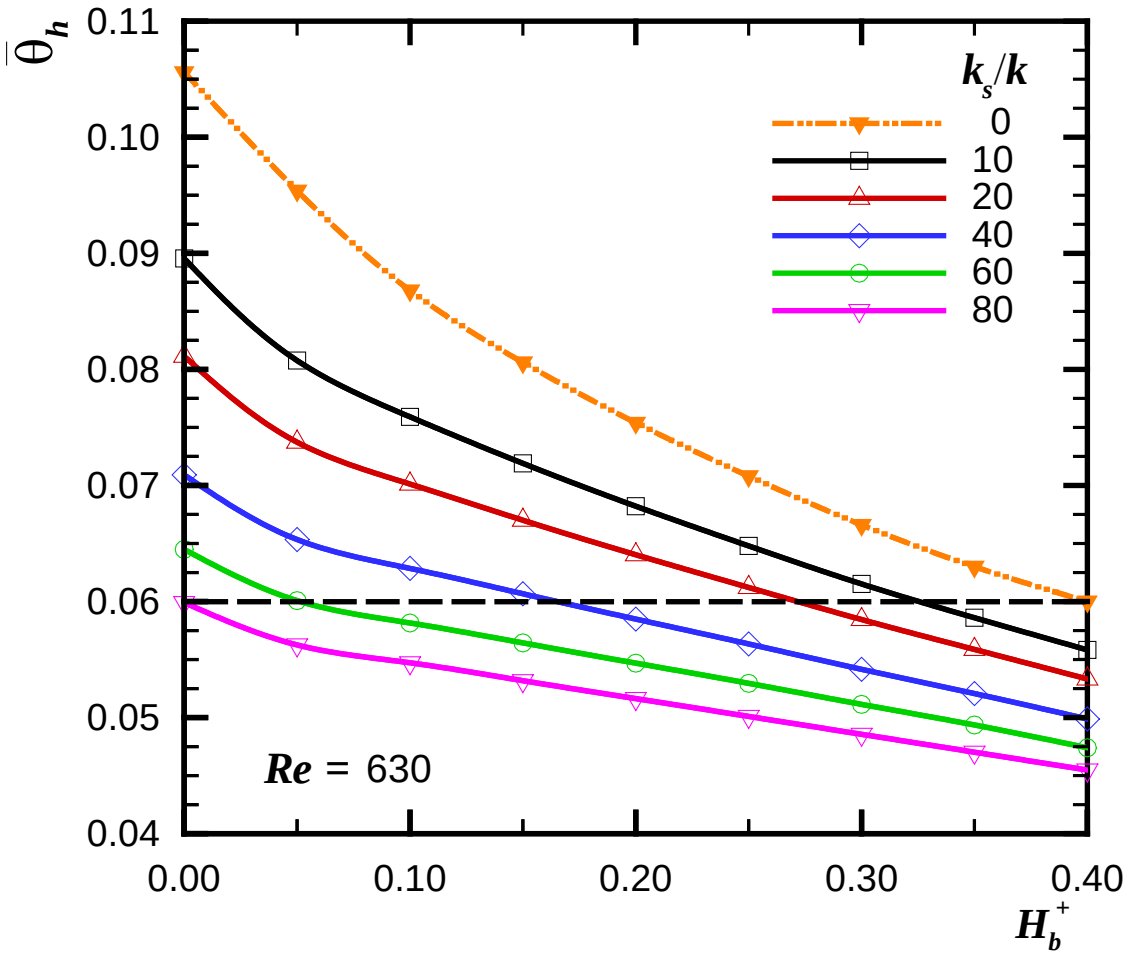

Figure 7 : Effect of the substrate thermal conductivity on $\overline{\theta}_h$ – *Re* = 630

- *Fixed Pressure Drop*

The results obtained under the constraint of a fixed pressure drop will be considered now. Five values of Δp^+ were selected so that the flow remained in the laminar regime. As shown in Fig. 8, for any heater height H_b^+ the flow rate (*Re*) increases with the pressure drop Δp^+, but for a fixed Δp^+ it decreases as the heater height H_b^+ increases, due to flow obstruction. The pumping power W_p^+ for a fixed Δp^+ is proportional to the flow rate, so that it is similar to the trends observed in Fig. 8 for the channel flow rate.

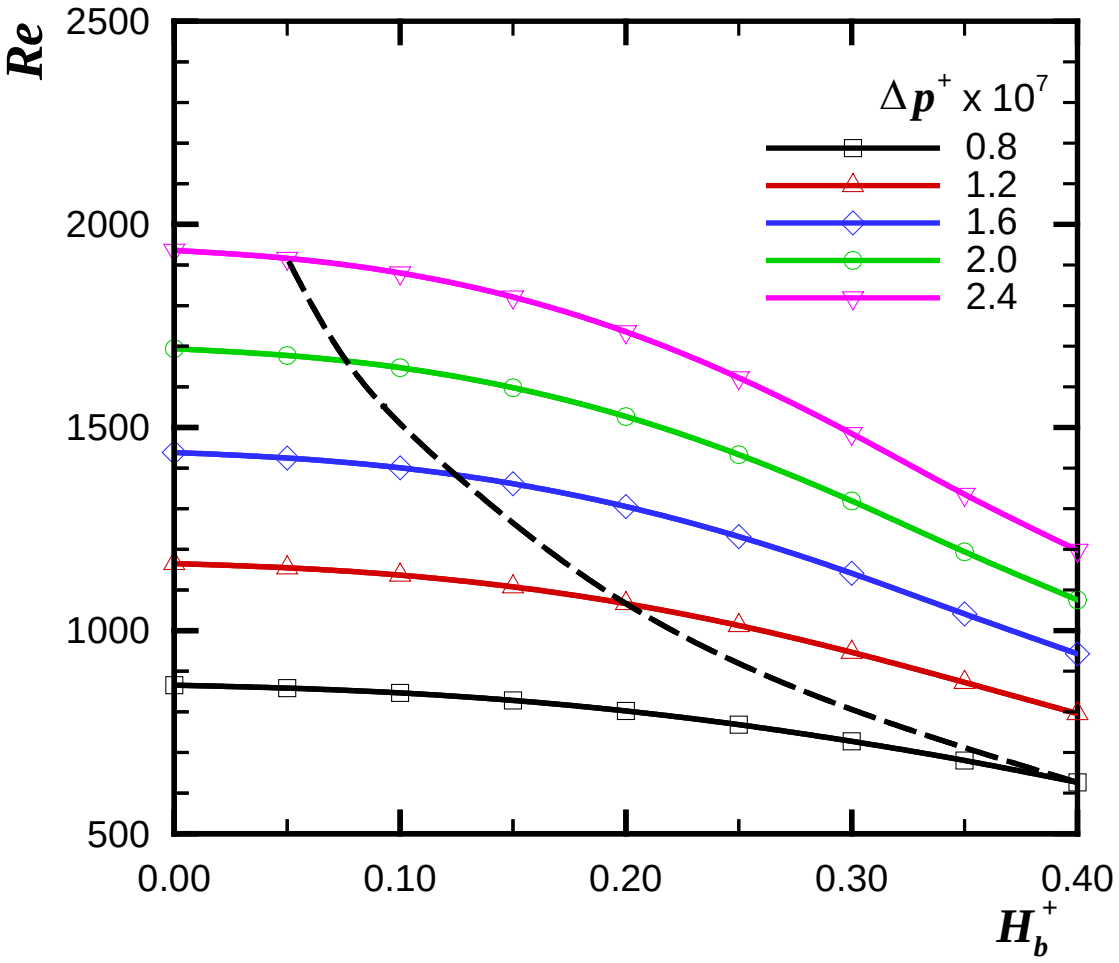

Figure 8 : Flow rate for fixed pressure drop

For an adiabatic substrate and the flow driven by a fixed pressure drop, the heater average temperature $\overline{\theta}_h$ is presented in Fig. 9, showing that within the investigated ranges of H_b^+ and *Re*, the temperature $\overline{\theta}_h$ decreases as the heater height increases. This figure also shows that for any heater height, the heater temperature decreases with the pressure drop due to larger channel flow rate. Considering again $\overline{\theta}_{h,max} = 0.06$, then the proper operating conditions are indicated by the region below the dashed line in Fig. 9. It shows that as the available pressure drop Δp^+ decreases, the minimum heater height must increase to provide a larger heat transfer area. The same dashed line is also indicated in Fig. 8, showing explicitly that as the minimum heater height increases, the channel mass flow rate for fixed pressure drop also decreases.

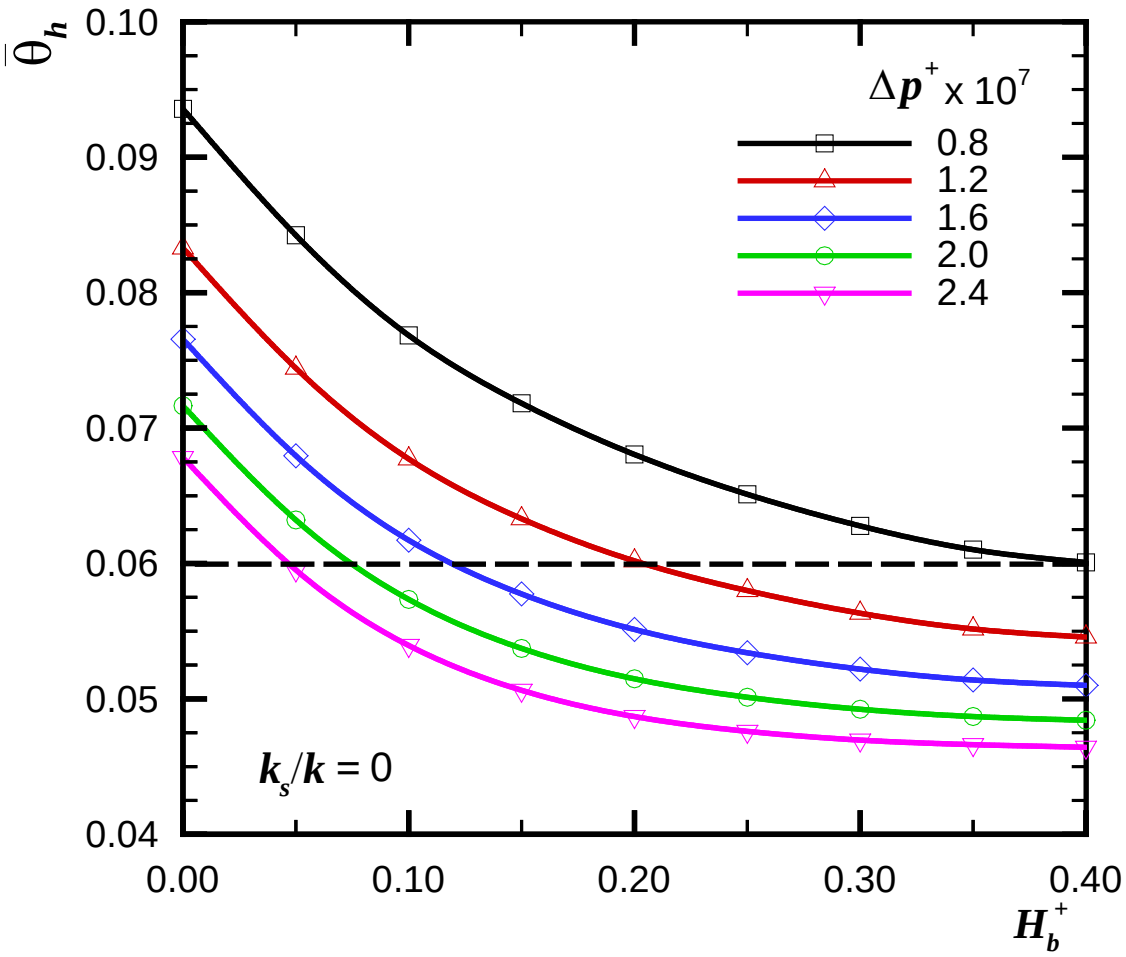

Figure 9 : Heater average temperature - fixed pressure drop and $(k_s/k) = 0$

When Δp^+ is fixed and the heater height increases, there are two opposing trends which determine the heater average temperature $\bar{\theta}_h$. One is a temperature decrease due to the increased heater area, and the other is just the opposite, a temperature increase due to the corresponding channel obstruction and flow rate decrease. The result of these opposite trends for $(k_s/k) = 0$ and $\Delta p^+ = 0.8\ 10^{-7}$ is presented in Fig. 10, showing that the heater attains a minimum average temperature $\bar{\theta}_h$ for $H_b^+ \cong 0.70$. As observed in this figure, for higher H_b^+, the channel obstruction causes a steep increase in $\bar{\theta}_h$.

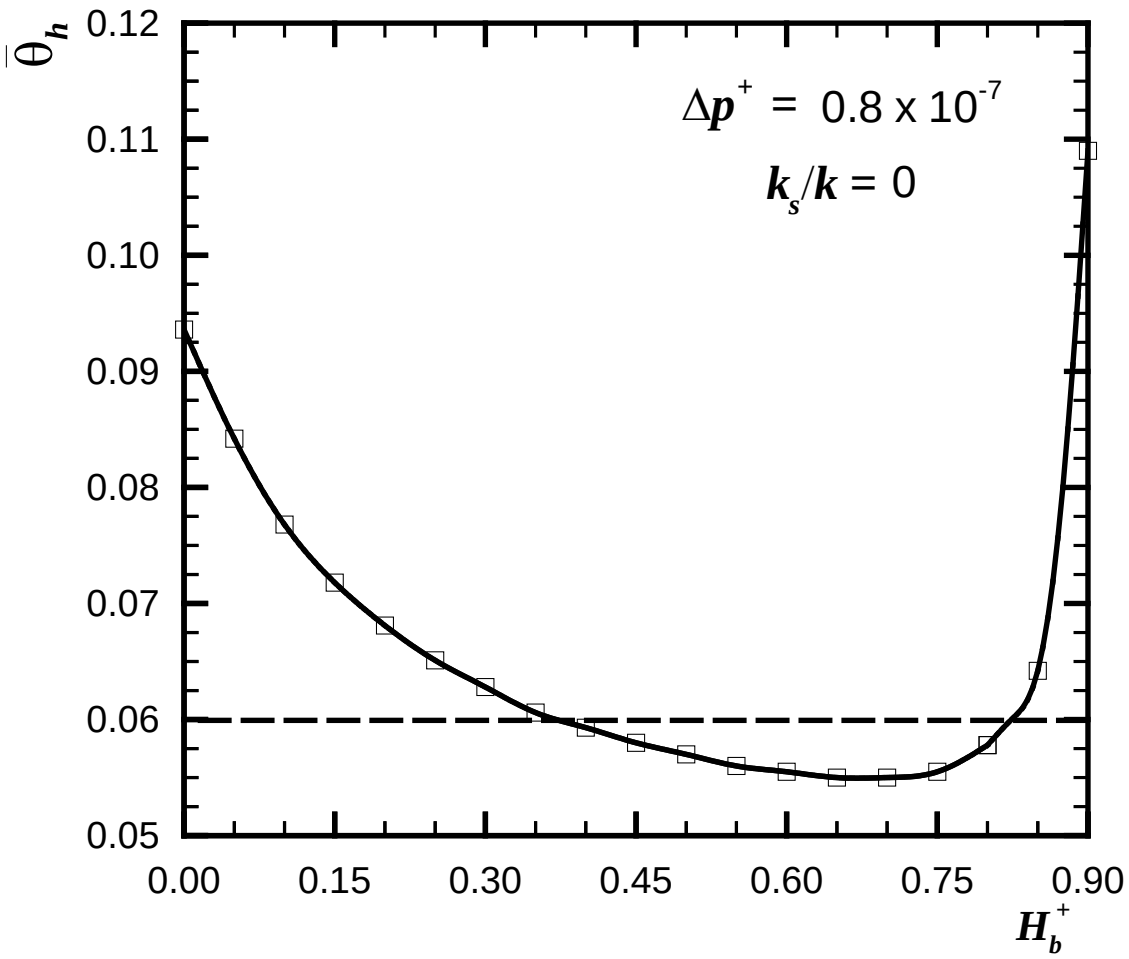

Figure 10 : Heater height for minimum temperature - fixed pressure drop and (k_s/k) = 0

The heater average temperature $\bar{\theta}_h$ for a conductive substrate with (k_s/k) = 80 is presented in Fig. 11 for the same fixed pressure drops Δp^+ used in Fig. 9. The trends are similar in both figures, but for the conductive substrate, due to the conjugate cooling, there is a substantial heater temperature decrease and a smaller relative change with the heater height H_b^+. Due to the conjugate cooling, the heater average temperature in Fig. 11 is below the considered limit of $\bar{\theta}_{h,max} = 0.06$ in all the investigated operating conditions.

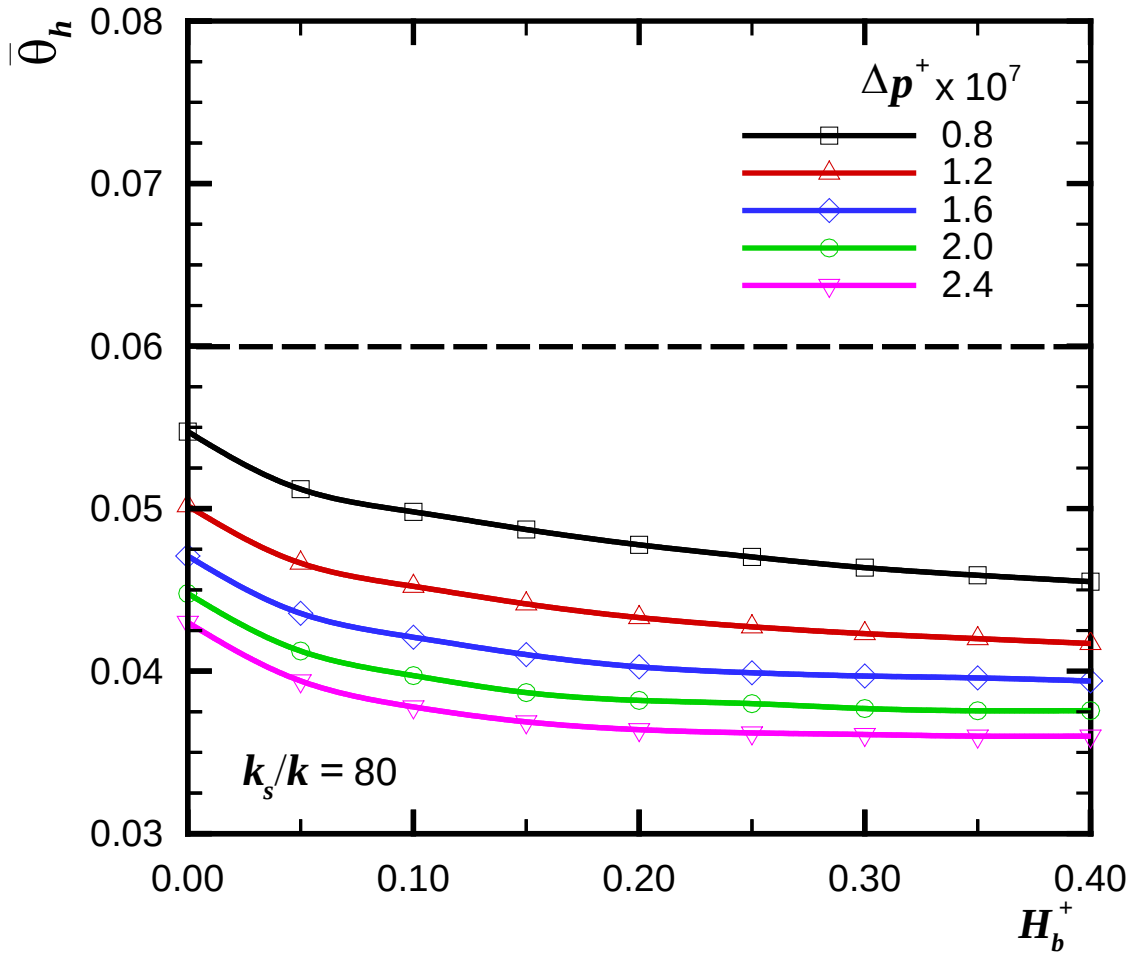

Figure 11 : Heater average temperature – fixed pressure drop and (k_s/k) = 80

- *Fixed Pumping Power*

When the channel flow is driven by a fixed pumping power, the product of the channel volumetric flow rate and the corresponding channel flow pressure drop remains constant. Thus, their change with the heater height must be opposite to each other. The results presented in Fig. 12 show the channel flow pressure drop Δp^+ for five distinct values of the dimensionless pumping power W_p^+, selected so that the resulting channel Re remained in the laminar regime. They show that for a fixed pumping power the pressure drop Δp^+ increases with the heater height and that for a given heater height it increases with the pumping power. Correspondingly, as mentioned, the channel flow rate for fixed pumping power must present an equivalent decrease with the heater height.

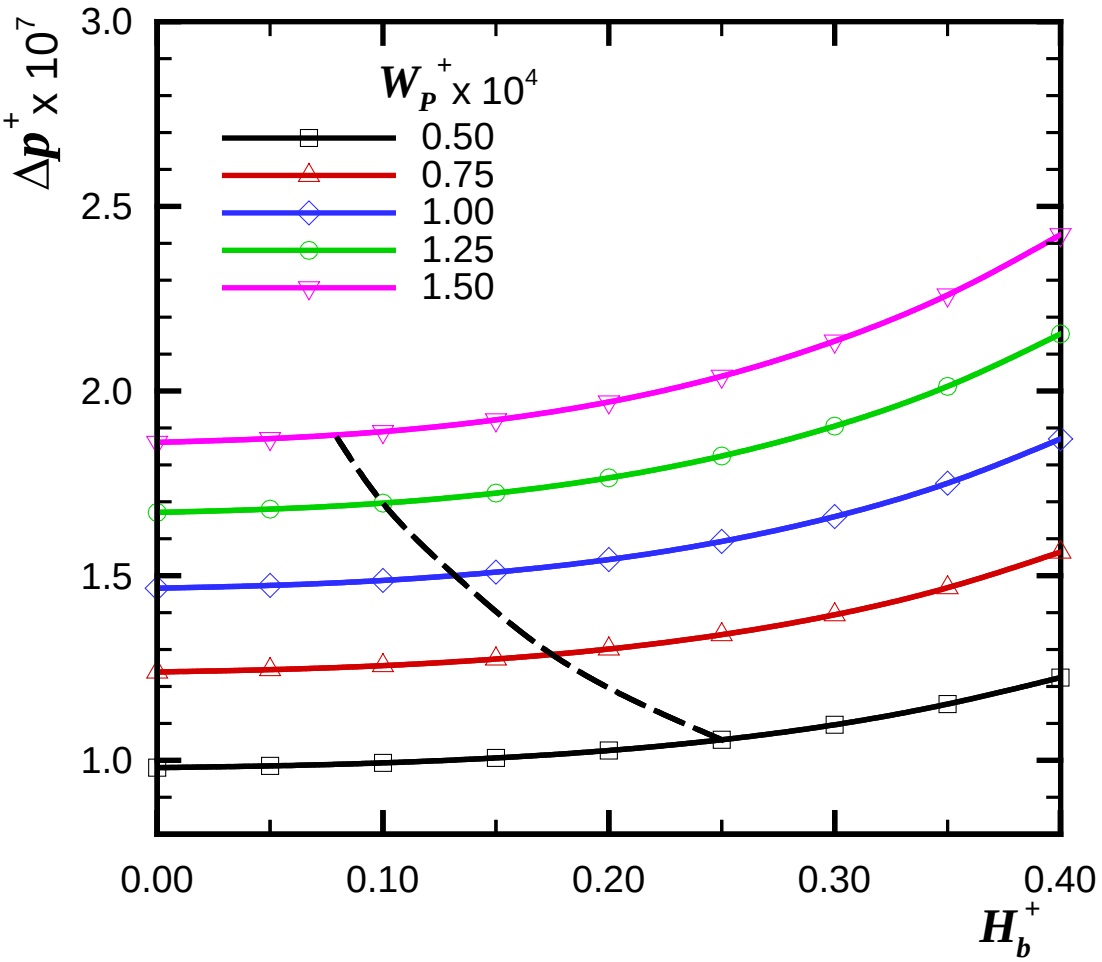

Figure 12 : Pressure drop for fixed pumping power

For an adiabatic substrate and the flow driven by fixed pumping power, Fig. 13 shows that the heater temperature $\overline{\theta}_h$ decreases as the heater height increases, while for a fixed heater height the temperature decreases with an increase of the pumping power, due respectively to an increased heat transfer area and a larger channel flow rate. Under fixed pumping power, an increase of the heater height H_b^+ increases the heat transfer area but reduces the channel flow rate. These two effects cause opposite trends on the heater temperature $\overline{\theta}_h$, so that this constraint also must present a heater height H_b^+ with minimum heater temperature. The curves drawn in Fig. 13 do not show the minimum because they were limited to $H_b^+ = 0.40$ due to the mentioned length of the flow recirculation zone downstream of the heater. The same heater temperature limit $\overline{\theta}_{h,max} = 0.06$ is presented as the dashed line in Fig. 13, indicating that the minimum needed heater height increases as the pumping power decreases. This dashed line is also presented in Fig. 12, indicating that when the fixed pumping power decreases, the channel flow rate and pressure drop decrease together and a taller heater is required to keep its average temperature below the maximum value.

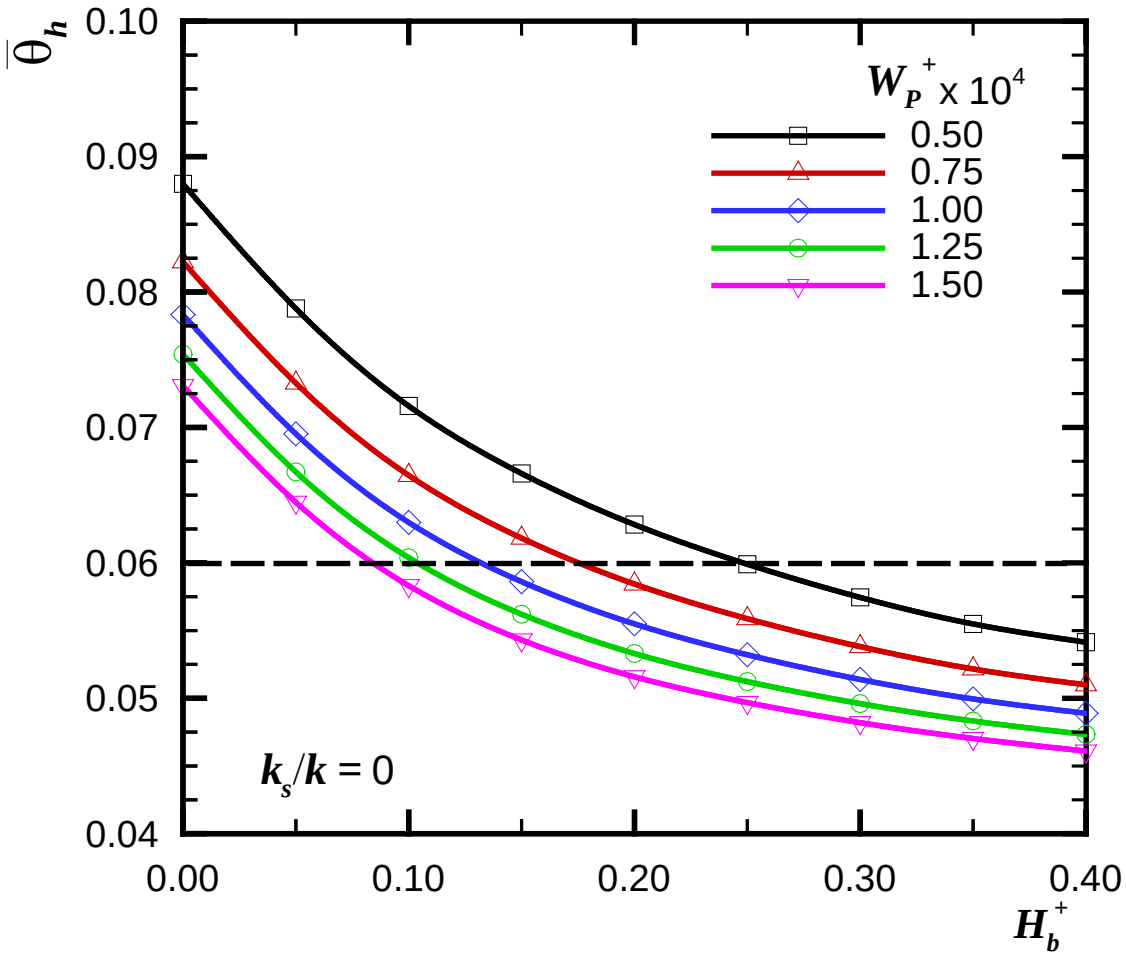

Figure 13 : Heater average temperature – fixed pumping power and $(k_s/k) = 0$

For a conductive substrate with $(k_s/k) = 80$, the resulting heater average temperature $\overline{\theta}_h$ is presented in Fig. 14 for fixed values of the dimensionless pumping power W_p^+. The trends are similar to those presented in Fig. 13, but this figure gives more evidence to the potential for the heat transfer enhancement obtained with the conductive substrate. The heater average temperature $\overline{\theta}_h$ in all the tested operating conditions was below the dashed line $\overline{\theta}_{h,max} = 0.06$. Considering for example the lower range of H_b^+ in Fig. 14, the values of $\overline{\theta}_h$ (or the heater global thermal resistance) are about 60 % of those for the adiabatic substrate (indicated in Fig. 13).

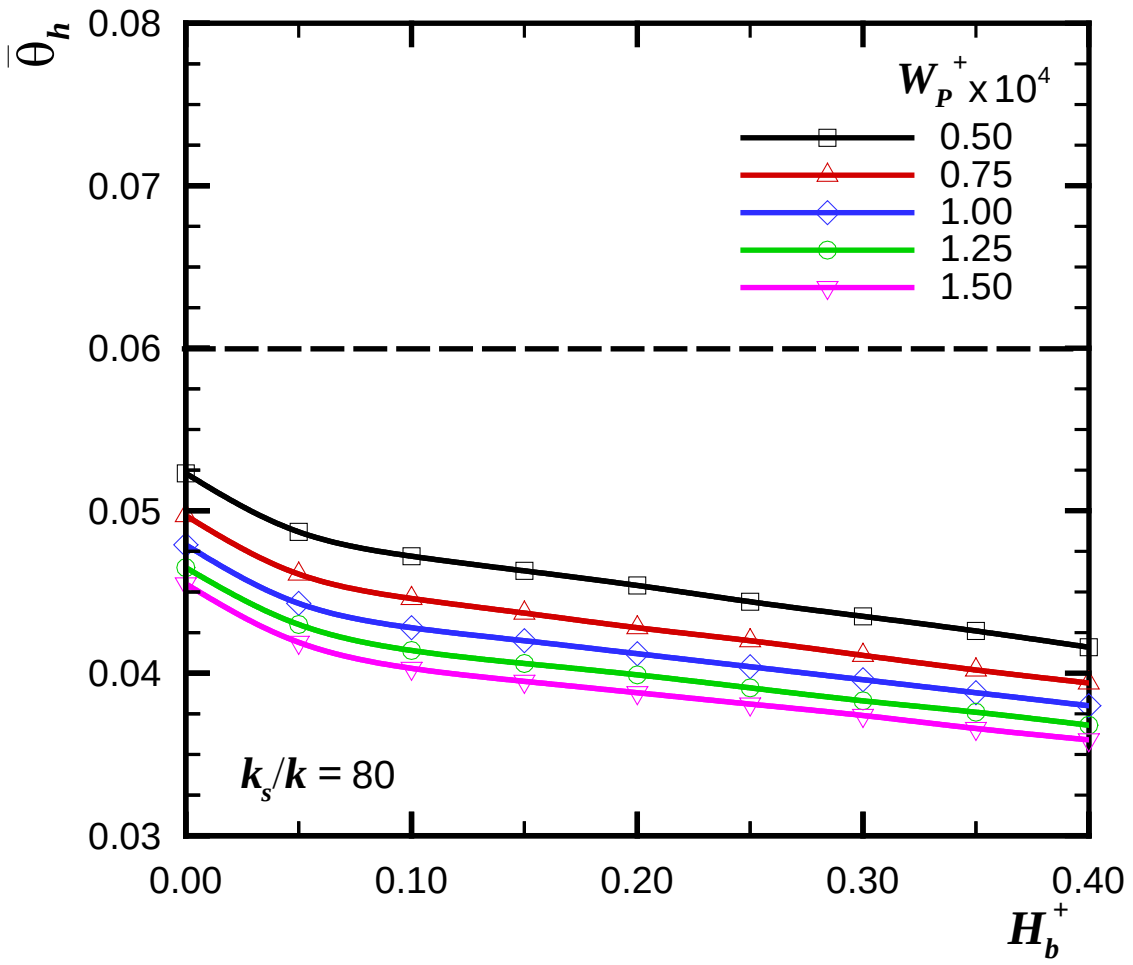

Figure 14 : Heater average temperature – fixed pumping power and (k_s/k) = 80

IV. Conclusions

The heater dimensionless average surface temperature (or its global thermal resistance) always decreased when either the airflow rate or the substrate plate thermal conductivity increased.

For a fixed flow rate, the heater temperature decreased as the heater height and the substrate thermal conductivity increased. Besides that, the flow pressure drop and the required pumping power increased with the heater height and the flow rate in the channel. In order to avoid that the flow recirculation zone downstream of the heater extended beyond the channel length at the largest *Re*, the relative heater height was limited to 0.40.

Under the constraints of a channel flow driven either by a fixed pressure drop or by a fixed pumping power, the flow rate decreased as the heater height increased, due to channel obstruction. In these cases there is a critical heater height which minimizes its thermal resistance to the airflow. The heater thermal resistance and temperature will increase with a heater height taller than this critical value. This behavior has no counterpart under the fixed flow rate constraint.

Under any flow constraint, considering an adiabatic substrate, there is a minimum heater height needed to keep it below a maximum allowable temperature. This required height decreases as the channel flow rate and the substrate thermal conductivity increase. In the present investigation, up to 50 per cent of the heater dissipation rate was spread by conduction through the substrate plate before returning to the airflow. This corroborates the potential of the conductive substrate to reduce the heater temperature or its global thermal resistance to the channel flow.

V. Acknowledgement

The support of CNPq (Brazilian National Research Council) to the first author is gratefully acknowledged.

- NOMENCLATURE

C = specific heat, J/kgK
C^+ = dimensionless unity thermal capacity
g = gravitational acceleration, m/s^2
Gr = Grashoff number
H = channel height, m
H_b = heater height, m

H_b^* = dimensionless heater height
H_b^+ = dimensionless heater height
L = total channel length, m
L_b = block heater length, m
L_d = channel downstream length, m
L_r = recirculation zone length downstream of the heater, m
L_u = channel upstream length, m
L_b^* = dimensionless heater length
L_r^+ = dimensionless recirculation zone length downstream of the heater
k = air thermal conductivity, W/mK
k_b = heater thermal conductivity, W/mK
k_s = substrate thermal conductivity, W/mK
k^+ = dimensionless thermal conductivity relative to air
P'_W = pumping power per unit depth, W/m
Pr = air Prandtl number
q' = heat generation per unit depth, W/m
q'_{cd} = heat conducted through the substrate plate per unit depth, W/m
q'' = heat flux, W/m^2
Re = Reynolds number, Eq. (1)
R'_t = global thermal resistance per unit depth, Eq. (8)
S^* = dimensionless volumetric source term, Eq. (6)
t = substrate thickness, m
T = temperature, K
u = x-velocity component, m/s
U = dimensionless x–velocity component
v = y-velocity component, m/s
V = dimensionless y–velocity component
x, y = Cartesian coordinates, Fig. 1, m
X, Y = dimensionless Cartesian coordinates
W_p^+ = dimensionless pumping power

a) Greek Symbols

β = coefficient of thermal expansion of the fluid, 1/K
Δp = pressure drop, Pa
Δp^* = dimensionless pressure drop
Δp^+ = dimensionless pressure drop
ρ = density, kg/m^3
θ = dimensionless temperature, Eq. (15)
υ = kinematic viscosity, m^2/s

b) Subscripts

h = heater
max = maximum value
0 = channel inlet

c) Superscripts

– = average

References Références Referencias

1. Ortega, A., Conjugate Heat Transfer in Forced Air Cooling of Electronic Components, in *Air Cooling Technology for Electronic Equipment*, eds. S.J. Kim and S.W. Lee, pp. 103-171, CRC Press, Boca Raton, FL, USA, 1996.
2. Nakayama, W., Forced Convective/Conductive Conjugate Heat Transfer in Microelectronic Equipment, *Annual Review of Heat Transfer*, vol. 8, pp. 1-45, 1997.
3. Ramadhyani, S., Moffat, D.F., and Incropera, F.P., Conjugate Heat Transfer From Small Isothermal Heat Sources Embedded in a Large Substrate, *International Journal of Heat and Mass Transfer*, vol. 28, pp. 1945-1952, 1985.
4. Davalath, J., and Bayazitoglu,Y., Forced Convection Cooling Across Rectangular Blocks, *Journal of Heat Transfer*, vol. 109, pp. 321-328, 1987.
5. Kim, S.H., and Anand, N.K., Laminar Heat Transfer Between a Series of Parallel Plates with Surface-Mounted Discrete Heat Sources, *Journal of Electronic Packaging*, vol. 117, pp. 522-62, 1995.
6. Kim, S.H., and Anand, N.K., Laminar Developing Flow and Heat Transfer Between a Series of Parallel Plates with Surface Mounted Discrete Heat Sources, *International Journal of Heat and Mass Transfer*, vol. 37, pp. 2231-2244, 1994.
7. Nakayama, W., and Park, S.H., Conjugate Heat Transfer From a Single Surface-Mounted Block to Forced Convective Air Flow in a Channel, *Journal of Heat Transfer*, vol. 118, pp. 301-309, 1996.
8. Nakamura, H., and Igarashi, T., Forced Convection Heat Transfer From a Low-Profile Block Simulating a Package of Electronic Equipment, *Journal of Heat Transfer,* vol. 126, pp. 463-470, 2004.
9. da Silva, A.K., Lorente, S., and Bejan, A., Optimal Distribution of Discrete Heat Sources on a Plate with Laminar Forced Convection, *International Journal of Heat and Mass Transfer*, vol. 47, pp. 2139-2148, 2004.
10. Icoz, T., Verna, N., and Jaluria, Y., Design of Air and Liquid Cooling Systems for Electronic Components Using Concurrent Simulation and Experiment, *Journal of Electronic Packaging,* vol. 128, pp. 466-478, 2006.
11. Zeng, Y., and Vafai, K., An Investigation of Convective Cooling of an Array of Channel-Mounted Obstacles, *Numerical Heat Transfer*, *Part A*, vol. 55, pp. 967-982, 2009.
12. Alves, T.A., Conjugate Cooling of Discrete Heaters in Channels (*in Portuguese*). Ph.D. Thesis, State University of Campinas, Brazil, 2010.
13. Kays, W.M., and Crawford, M.E., *Convective Heat and Mass Transfer*, McGraw-Hill, New York, USA, 1993.

14. Patankar, S.V., *Numerical Heat Transfer and Fluid Flow*, Hemisphere, Washington, D.C., USA, 1980.
15. De Vahl Davis, G., Natural Convection of Air in a Square Cavity: A Benchmark Numerical Solution, *International Journal for Numerical Methods in Fluids*, vol. 3, pp. 249-264, 1983.

This page is intentionally left blank